

The synaptic blocker botulinum toxin A decreases the density and complexity of oligodendrocyte precursor cells in the adult mouse hippocampus

Irene Chacon-De-La-Rocha¹ | Gemma L. Fryatt² | Andrea D. Rivera^{1,3} | Laura Restani⁴ | Matteo Caleo^{4,5} | Diego Gomez-Nicola² | Arthur M. Butt¹ 

¹Institute of Biomedical and Biomolecular Sciences, School of Pharmacy and Biomedical Sciences, University of Portsmouth, Portsmouth, UK

²Centre for Biological Sciences, University of Southampton, Southampton, UK

³Department of Neuroscience, Institute of Human Anatomy, University of Padua, Padua, Italy

⁴National Research Council, Neuroscience Institute, Pisa, Italy

⁵Department of Biomedical Sciences, University of Padua, Padua, Italy

Correspondence

Diego Gomez-Nicola, Centre for Biological Sciences, University of Southampton, Southampton, UK.
Email: d.gomez-nicola@soton.ac.uk

Arthur M. Butt, Institute of Biomedical and Biomolecular Sciences, School of Pharmacy and Biomedical Sciences, University of Portsmouth, Portsmouth, UK.
Email: Arthur.butt@port.ac.uk

Funding information

BBSRC, Grant/Award Number: BB/M029379/1; MRC, Grant/Award Number: MR/P025811/1; Alzheimer's Research UK, Grant/Award Number: PG2014B-2; University of Portsmouth; CNR - Joint Laboratories

Abstract

Oligodendrocyte progenitor cells (OPCs) are responsible for generating oligodendrocytes, the myelinating cells of the CNS. Life-long myelination is promoted by neuronal activity and is essential for neural network plasticity and learning. OPCs are known to contact synapses and it is proposed that neuronal synaptic activity in turn regulates their behavior. To examine this in the adult, we performed unilateral injection of the synaptic blocker botulinum neurotoxin A (BoNT/A) into the hippocampus of adult mice. We confirm BoNT/A cleaves SNAP-25 in the CA1 area of the hippocampus, which has been proven to block neurotransmission. Notably, BoNT/A significantly decreased OPC density and caused their shrinkage, as determined by immunolabeling for the OPC marker NG2. Furthermore, BoNT/A resulted in an overall decrease in the number of OPC processes, as well as a decrease in their lengths and branching frequency. These data indicate that synaptic activity is important for maintaining adult OPC numbers and cellular integrity, which is relevant to pathophysiological scenarios characterized by dysregulation of synaptic activity, such as age-related cognitive decline, Multiple Sclerosis and Alzheimer's disease.

KEYWORDS

BoNT/A, botulinum toxin A, hippocampus, mouse, oligodendrocyte progenitor cell, RRID:AB_143165, RRID:AB_2313606, RRID:AB_2340613, RRID:AB_11213678, RRID:SCR_002798, RRID:SCR_003070, RRID:SCR_016788, RRID:SCR_017348, SNAP-25, SNARE, Synapse

Abbreviations: AD, Alzheimer's disease; BoNT/A, botulinum neurotoxin A; Cspg4, chondroitin sulfate proteoglycan 4 (NG2); EM, electron microscopy; FOV, field of view; GABA, gamma aminobutyric acid; h, hours; min, minutes; MS, multiple sclerosis; NG2, neuron-glia 2 (Cspg4); OPCs, oligodendrocyte progenitor cells; PBS, phosphate-buffered saline; SD, standard deviation; SNAP, synaptosomal-associated protein; SNARE, soluble N-ethylmaleimide-sensitive factor-attachment protein receptors; TTX, tetrodotoxin.

Irene Chacon-De-La-Rocha and Gemma L. Fryatt contributed equally to the paper.

Edited by Stephen Crocker and Cristina Ghiani. Reviewed by Jack Antel and David Martinelli.

This is an open access article under the terms of the Creative Commons Attribution License, which permits use, distribution and reproduction in any medium, provided the original work is properly cited.

© 2021 The Authors. Journal of Neuroscience Research published by Wiley Periodicals LLC.

1 | INTRODUCTION

Oligodendrocyte progenitor cells (OPCs) are a significant population of cells in the adult brain with the fundamental function of life-long generation of oligodendrocytes, which is required to myelinate new connections formed in response to new life experiences and to replace myelin lost through natural “wear and tear” and disease (Hill et al., 2018; Young et al., 2013; Zawadzka et al., 2010). OPCs are identified by their expression of the proteoglycan NG2 (Cspg4) (Ong & Levine, 1999; Stallcup, 1981) and have a complex morphology, extending processes to contact neuronal synapses and nodes of Ranvier, sensing neuronal glutamatergic and GABAergic activity (Bergles et al., 2000; Butt et al., 1999; Hamilton et al., 2010; Kukley et al., 2007; Lin & Bergles, 2004; Ziskin et al., 2007). Several lines of evidence indicate neuronal synaptic activity regulates OPC proliferation and differentiation (Fannon et al., 2015; Hamilton et al., 2017; Mangin et al., 2012; Zonouzi et al., 2015). Optogenetic studies have shown that neuronal activity stimulates OPC proliferation and differentiation in the cerebral cortex (Gibson et al., 2014). Furthermore, motor learning has been shown to drive OPC differentiation, and failure to generate new oligodendrocytes impairs myelination of newly formed neuronal connections and learning ability (McKenzie et al., 2014; Xiao et al., 2016). Hence, it is proposed that decreased synaptic activity may result in disruption of OPC regenerative capacity in neurodegenerative diseases, such as Multiple Sclerosis (MS) and Alzheimer's disease (AD) (Chacon-De-La-Rocha et al., 2020; Rivera et al., 2016; Vanzulli et al., 2020).

The synaptic protein SNAP-25 is necessary for synaptic vesicle fusion and its cleavage by botulinum neurotoxins (BoNTs) blocks neurotransmitter release and synaptic signaling (Caleo & Restani, 2018). Developmental myelination is inhibited by ablation of neuronal SNAP-25 either by BoNT/A in cell culture (Wake et al., 2011), or genetically *in vivo* (Korrell et al., 2019), but the effects of synaptic activity on adult OPCs remain unclear. In the present study, we investigated the effects of prolonged synaptic silencing on adult OPCs, by local injection of botulinum neurotoxin A (BoNT/A) into the mouse hippocampal CA1 region, which has been demonstrated to produce a sustained blockade of synaptic transmission via cleavage of the synaptic protein SNAP-25 (Antonucci et al., 2008; Caleo & Restani, 2018; Caleo et al., 2012). Our results demonstrate that the synaptic blocker BoNT/A decreases the density and complexity of OPCs, leading to overall cellular atrophy. These results indicate synaptic activity is important in the long-term maintenance of the population of OPCs, with relevance for understanding pathological process leading to progressive demyelination.

2 | MATERIALS AND METHODS

2.1 | Ethics statement

All procedures were performed in compliance with the EU Council Directive 2010/63/EU on the protection of animals used for

Significance

Oligodendrocyte progenitor cells (OPCs) are responsible for life-long myelination, which is essential for higher cognitive function. OPCs are renowned for sensing neuronal synaptic activity, which regulates adaptive myelination and underpins learning and cognitive function. This study shows that silencing synaptic activity induces OPC atrophy in the hippocampus and has important implications for the loss of cognitive function associated with aging and neuropathology.

scientific purposes, and approved by the Italian Ministry of Health (protocol # 346/2013-B). All surgical procedures were performed under deep anesthesia and all efforts were made to ameliorate suffering of animals.

2.2 | Animals and tissues

C57BL/6N mice were bred and group housed in the animal facility of the CNR Neuroscience Institute in Pisa (Italy). Mice were housed in groups of 4 to 10, under a 12 hr light/dark cycle at 21°C, with food and water *ad libitum*, and experimental groups contained a spread of sexes. Eight mice aged 11–12 weeks were anesthetized by intraperitoneal injection of Avertin (20 ml/kg, 2,2,2-tribromoethanol solution; Sigma-Aldrich, Cat. #T48402) and mounted in a stereotaxic frame (David Kopf Instruments, Tujunga, CA), for injection of BoNT/A ($n = 4$ mice) or sterile vehicle ($n = 4$ mice). The isolation and purification of BoNT/A was performed in house, as previously described (Schiavo & Montecucco, 1995; Shone & Tranter, 1995), and its activity assayed and characterized in the hippocampal model (Antonucci et al., 2008; Caleo et al., 2012) (Figure 1). In brief, BoNT/A was isolated from cultures of *Clostridium botulinum* and purified as 150 kDa di-chain neurotoxin, as described by (Shone & Tranter, 1995) and (Schiavo & Montecucco, 1995). After purification, toxin was dialyzed in 10 mM TrisCl, 150 mM NaCl, pH 6.8 and stored at -80°C until use. For hippocampal injections, stock of toxin (50 nM) was thawed on ice, diluted to working concentration (1nM, in 2% rat serum albumin, PBS) and kept on ice until briefly warming to hand temperature immediately prior to brain injections. For hippocampal injections, a stereotaxically guided injection of BoNT/A (0.2 μl of a 1 nM solution) or vehicle (2% rat serum albumin in PBS) was made into the dorsal hippocampus using fine glass micropipettes (at the coordinates, in mm with respect to the Bregma, A-P -2.0 , M-L 1.5, H 1.7 below the dura), as previously characterized (Antonucci et al., 2008; Caleo et al., 2012). The experiments were designed in compliance with ARRIVE guidelines and no mice were excluded from analyses. In all injected animals, recovery was uneventful and no overt behavioral abnormalities were observed. Two weeks after injections, mice were deeply anesthetized with chloral hydrate and perfused through the

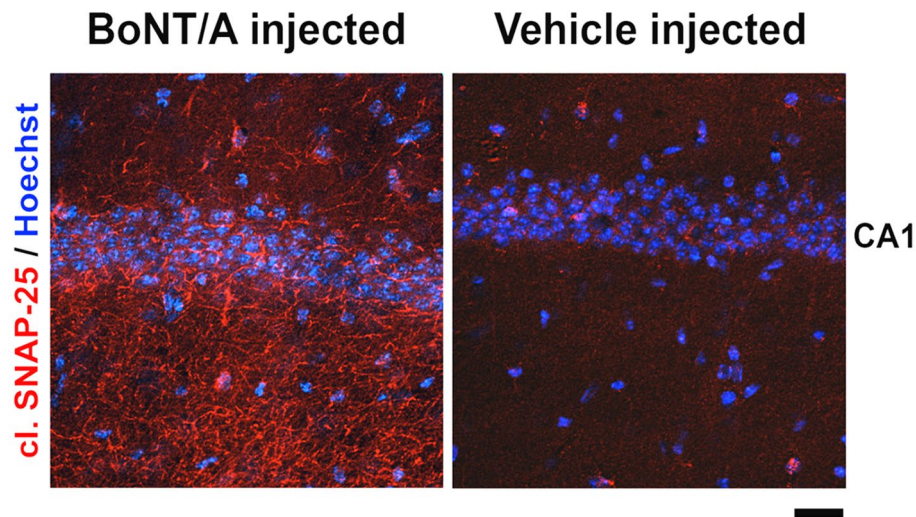


FIGURE 1 BoNT/A cleaves SNAP-25 in the hippocampus. Representative fluorescence micrographs of coronal sections of the adult mouse hippocampus illustrating the CA1 area following stereotaxical injection of BoNT/A or vehicle. Sections are immunolabeled with an antibody specific for BoNT/A-truncated SNAP-25 (red), which has been thoroughly characterized in previous studies (Antonucci et al., 2008; Caleo et al., 2012), and counterstained with Hoechst nuclear dye. Scale bar = 100 μm ; images representative of two sections each from four animals [Color figure can be viewed at wileyonlinelibrary.com]

heart with freshly prepared 4% paraformaldehyde in 0.1 M phosphate buffer (PB), and the brains processed for immunohistochemistry (see below).

2.3 | Immunohistochemistry

Brains were post-fixed for 1 hr at 4°C and brain sections (50 μm thick) were cut with a freezing microtome and stored at 4°C until use in cryoprotectant solution containing 25% sucrose and 3.5% glycerol in 0.05 M PBS (all chemicals from Sigma-Aldrich, unless otherwise stated), at pH 7.4, prior to immunostaining (for details of antibodies, see Table 1). To detect SNAP-25 cleavage, we used a rabbit polyclonal antibody specific for BoNT/A-truncated SNAP-25 (gift from Prof Ornella Rossetto, University of Padua); antibody raised against the immunizing sequence CKADSNKTRIDEANQ (aa 184–197), affinity purified and previously characterized with full controls in our previous studies (Antonucci et al., 2008; Caleo et al., 2012). Sections were blocked with 10% donkey serum in PBS containing 0.25% Triton X-100 and then incubated overnight at room temperature with the anti-cleaved SNAP-25 antibody (1:500 dilution). On the following day, sections were incubated with anti-rabbit Rhodamine Red X, 1:500 (Jackson ImmunoResearch Labs Cat# 711-295-152, RRID:AB_2340613), washed in PBS, counterstained with Hoechst 33342 (Thermo Fisher Scientific Cat#62249). For NG2 immunostaining, sections were blocked with 0.5% bovine serum albumin (BSA) for 1–2h, washed three times in PBS, and incubated overnight in the antibody solution which comprised of the primary antibody rabbit anti-NG2, 1:500 (Millipore Cat# AB5320, RRID:AB_11213678), diluted in blocking solution containing 0.25% Triton-X. Tissues were then washed three times in PBS and incubated for 1–2h with appropriate fluorochrome secondary antibody, diluted at 1:500 in

blocking solution (Alexa Fluor 488-AffiniPure Goat Anti-Rabbit IgG (H+L), Thermo Fisher Scientific Cat# A-11008, RRID:AB_143165), or biotinylated secondary antibody, diluted at 1:200 in blocking solution (Biotinylated Goat Anti-Rabbit IgG (H+L), Vector Laboratories Cat# BA-1000, RRID:AB_2313606). Finally, sections were washed three times with PBS before being mounted on glass slides and covered with mounting medium and glass coverslips ready for imaging.

2.4 | Imaging and analysis

Immunofluorescence images were captured using a Zeiss Axiovert LSM 710 VIS40S confocal microscope and maintaining the acquisition parameters constant to allow comparison between samples within the same experiment. Acquisition of images for cell counts was performed with $\times 20$ objective. Images for OPC reconstruction were taken using $\times 100$ objective and capturing z-stacks formed by 80–100 single planes with an interval of 0.3 μm . All analyses were performed by a person who was blind to experimental conditions and no exclusion criteria were applied. OPC cell counts were performed manually on images using a constant field of view (FOV) of 200 $\mu\text{m} \times 200 \mu\text{m}$ centered on the CA1 area, and data expressed as OPC density per mm^2 ; data from two sections per mouse were averaged, to provide a final $n = 4$ mice per treatment group, on which statistics were performed. To determine the process domains (cell coverage) of OPCs, chromogenic NG2 immunostained sections were examined on an Olympus dotSlide digital slide scanning system based on a BX51 microscope stand with an integrated scanning stage and Olympus CC12 color camera, and the cell coverage of OPCs was measured using ImageJ by drawing a line around the entire cell process field and the area within the line was measured using ImageJ (RRID:SCR_003070), and data were expressed as μm^2 ;

TABLE 1 List of antibodies used

Antibody	Supplier information	RRID	Immunogen	Dilution
Cleaved SNAP-25	Custom made by Prof Ornella Rossetto (University of Padua) See Antonucci et al. (2008), for testing and full controls (Figure 1b–d) Rabbit polyclonal (affinity purified)	From Prof Ornella Rossetto (University of Padua)	Immunizing sequence: CKADSNKTRIDEANQ (aa 1 84-197)	1:500
Anti-NG2 Chondroitin Sulfate Proteoglycan antibody	Millipore Rabbit polyclonal Cat# AB5320	RRID:AB_11213678	Immunoaffinity purified NG2 Chondroitin Sulfate Proteoglycan from rat	1:500
Goat anti-Rabbit IgG (H+L) Cross-Adsorbed Secondary Antibody, Alexa Fluor 488	Thermo Fisher Scientific Goat polyclonal Cat# A-11008	RRID:AB_143165	IgG (H+L), anti-IgG (H+L)	1:500
Goat Anti-Rabbit IgG Antibody (H+L), Biotinylated	Vector Laboratories Goat polyclonal Cat# BA-1000	RRID:AB_2313606	IgG (H+L), anti-IgG (H+L)	1:200
Rhodamine Red-X-AffiniPure Donkey Anti-Rabbit IgG (H+L) (min X Bov, Ck, Gt,GP, Sy Hms, Hrs, Hlu, Ms, Rat, Shp Sr Prot) antibody	Jackson ImmunoResearch Labs Donkey polyclonal Cat# 711-295-152	RRID:AB_2340613	Rabbit IgG (H+L)	1:500

data from two sections per mouse were averaged, to provide a final $n = 4$ mice per treatment group, on which statistics were performed. For detailed morphological analysis of single OPCs, cells were drawn using NeuroLucida 360 (MBF Bioscience, RRID:SCR_016788), and their morphology was analyzed using NeuroLucida 360 explorer (MBF Bioscience, RRID:SCR_017348) for measurements of the number of processes per cell, process lengths, number of process terminals (end points), and number of nodes (branch points); three cells were drawn from the center of the CA1 field in one section per mouse (12 cells from 4 mice per treatment group), and data were averaged in each mouse, to provide a final $n = 4$ mice per treatment group, on which statistics were performed. Sholl analysis was performed on the same cells, using a $5\mu\text{m}$ interval between Sholl shells ($n = 12$ cells from four mice in each experimental group).

2.5 | Statistical analysis

All data are represented as mean \pm SD. Data sets were analyzed statistically by Graphpad Prism 6.0 software (Graphpad, San Diego, USA, RRID:SCR_002798). Statistical differences between two parametric samples were measured by the unpaired two tailed Student's t test, and statistical differences of multiple parameters were assessed by

two-way ANOVA with Sidak's post hoc multiple comparisons test. Statistics, actual p values, when significant, and number of samples are reported in the text. Data were analyzed by a person who was blind to experimental conditions and no exclusion criteria were applied. Statistical significance in the figures is indicated as: * $p \leq 0.05$; ** $p \leq 0.01$; *** $p \leq 0.001$; **** $p \leq 0.0001$, ns = $p > 0.05$.

3 | RESULTS

3.1 | The synaptic blocker BoNT/A causes a reduction in OPC numerical density and size in the CA1 region of the hippocampus

The long-term effects of synaptic silencing on adult OPCs have not been previously studied. We addressed this by injecting adult mice into the left hippocampus with BoNT/A (1 nM solution, 0.2 μl), which causes persistent blockade of hippocampal synaptic activity for up to 120 days (Antonucci et al., 2008; Caleo et al., 2012). The hippocampus was analyzed 2 weeks post-injection and we confirmed that BoNT/A mediates long-term SNAP-25 cleavage in the CA1 area of inoculated side (Figure 1), which has been detailed comprehensively in earlier studies, by immunohistochemistry and western

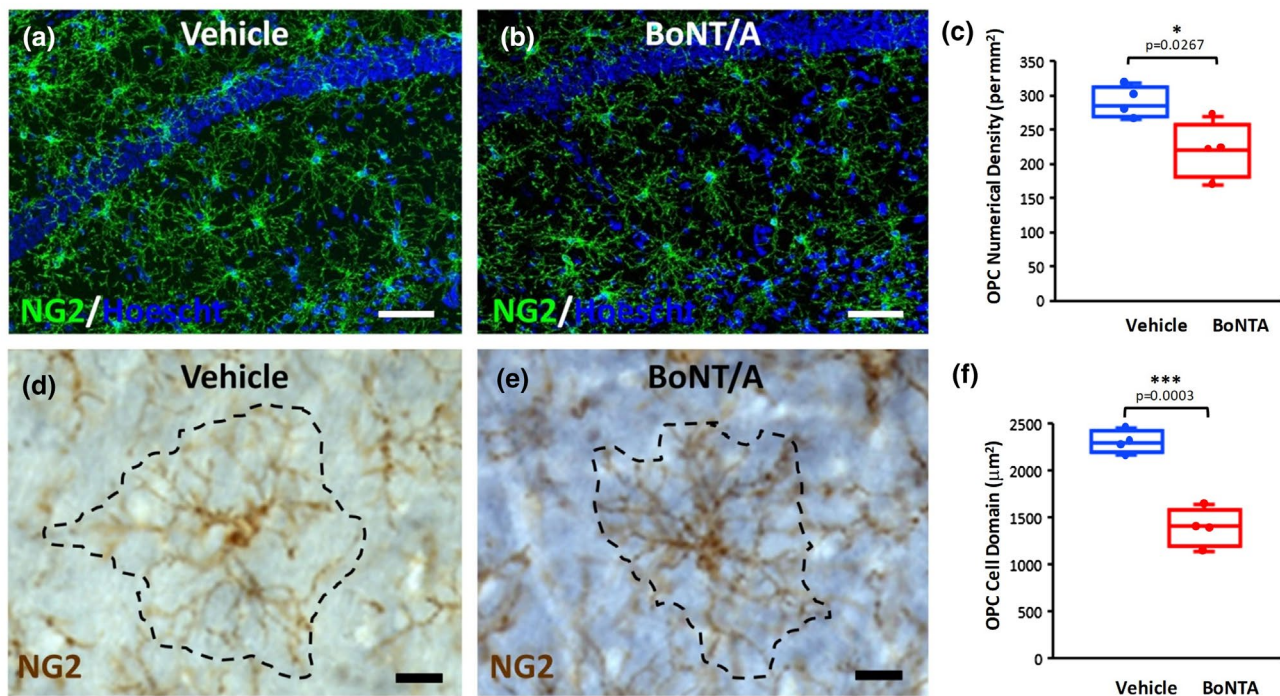


FIGURE 2 Effect of synaptic silencing with BoNT/A on adult hippocampal OPC *in vivo*. Analysis of OPCs in hippocampus following injection with BoNT/A to silence synaptic activity, or vehicle in controls. (a–c) Immunofluorescence labeling for NG2 (green) and counterstain with Hoechst nuclear dye (blue), illustrating the overall distribution of OPCs in the CA1 area of the hippocampus following injection of vehicle (a) or BoNT/A (b), together with box-whisker plots of the numerical density of OPCs in the CA1 (c); scale bars = $50\mu\text{m}$; data were averaged from two sections per mouse to provide a mean \pm SEM from $n = 4$ mice per treatment group; $p = 0.0267$, unpaired t test. (d–f) High magnification of individual chromogenic NG2 immunolabeled OPCs in the CA1 area of the hippocampus illustrating their process domains (broken lines) following injection of vehicle (d) or BoNT/A (e), together with box-whisker plots of OPC cell domains (f); scale bars = $20\mu\text{m}$; data were averaged from two sections per mouse (37 cells for vehicle, 43 cells for BoNT/A), to provide a mean \pm SEM from $n = 4$ animals per treatment group; $p = 0.0003$, unpaired t test [Color figure can be viewed at wileyonlinelibrary.com]

blot (Antonucci et al., 2008; Caleo et al., 2012). Next, we used immunolabeling for NG2 to identify OPCs (Butt et al., 1999), and we focused on the CA1 area as OPCs had been previously shown to form synapses with neurones and respond to synaptic signaling in this area (Bergles et al., 2000; Lin & Bergles, 2004). Confocal images demonstrate an evident decrease in NG2 immunostaining 14 days after BoNT/A injection (Figure 2a), compared to controls injected with vehicle (Figure 2b). Quantification confirmed OPC numerical density was decreased following BoNT/A injection compared to controls (Figure 2c; unpaired *t* test, $t = 2.918$, $df = 6$, $p = 0.0267$; data from two sections per mouse were averaged, to provide a final $n = 4$ mice per treatment group). Moreover, mapping the process domains of individual OPCs (Figure 2d,e) demonstrated these were significantly reduced following synaptic silencing (Figure 2f; unpaired *t* test, $t = 7.651$, $df = 6$, $p = 0.0003$; data from 37 cells for vehicle and 43 cells for BoNT/A from two sections per mouse were averaged, to provide a final $n = 4$ mice per treatment group). The data show that the synaptic blocker BoNT/A results in a decline in the overall number of OPC and those that persist display a marked shrinkage.

3.2 | BoNT/A decreases the morphological complexity of OPCs

Adult OPCs respond to pathology by changes in their morphology (Butt et al., 2002), and in the adult hippocampus they react to toxic activation of glutamatergic receptors by extending a greater number of short process (Ong & Levine, 1999). We therefore examined OPC morphology in detail using NeuroLucida (Figure 3) and Sholl analysis (Figure 4). Overall, OPCs had a characteristic complex morphology in vehicle-injected controls, with on average 12 primary processes that extended radially for 50–100 μm from a central cell body (Figure 3a). In comparison, OPCs displayed overall atrophy following BoNT/A injection, with an evident decrease in cellular complexity (Figure 3b); the shrinkage of the OPC process field following BoNT/A treatment is amplified in the *y*-plane (upper insets, Figure 3a,b), and in the *x*-plane OPCs in controls are seen to have a dense network of branching processes, which is stunted following synaptic silencing (lower insets, Figure 3a,b). Multiple parameters of process complexity were quantified (Figure 3c–e); data were from three cells drawn from the center of the CA1 field in one section per mouse, which was averaged in each mouse, to provide a final $n = 4$ mice per treatment group. There were significant decreases in the number of processes extending from the cell body following BoNT/A injection, ranging from 2 to 12, compared to 8–25 in controls (Figure 3c; unpaired *t* test, $p = 0.0448$, $t = 2.528$, $df = 6$, $n = 4$ animals in each group), together with significant decreases in the length of processes from each cell (Figure 3d; unpaired *t* test, $p = 0.0116$, $t = 3.582$, $df = 6$, $n = 4$ animals in each group), as well as the number of process terminals, or end points (Figure 3e; unpaired *t* test, $p = 0.0280$, $t = 2.881$, $df = 6$, $n = 4$ animals in each group), and the number of branch points along processes (nodes) (Figure 3f; unpaired *t* test, $p = 0.0277$, $t = 2.891$, $df = 6$, $n = 4$ animals in each

group). The results indicate a primary effect of BoNT/A on cellular branching and this was examined further by Sholl analysis (Figure 4). The data indicate that following synaptic silencing the most marked changes in OPC processes were within 20–30 μm of the cell body, with significant decreases in the number of nodes, or branch points (Figure 4b; two-way ANOVA followed by Sidak's multiple comparisons tests, $F(13, 308) = 90.49$, $p < 0.0001$, $n = 12$ cells from four animals in each group), as well as the number of process terminals (Figure 4c; two-way ANOVA followed by Sidak's multiple comparisons tests, $F(13, 308) = 98.22$, $p < 0.0001$, $n = 12$ cells from four animals in each group), and the lengths of processes (Figure 4d; two-way ANOVA followed by Sidak's multiple comparisons tests, $F(13, 308) = 182.1$, $p < 0.0001$, $n = 12$ cells from four animals in each group). In addition, we analyzed the processes length in the different branch orders, identifying that synaptic silencing primarily caused shrinkage of the distal branches, and the maximum branch order was decreased to 13 compared to 15 in controls (Figure 4e; two-way ANOVA followed by Sidak's multiple comparisons tests, $F(15, 352) = 94.80$, $p < 0.0001$, $n = 12$ cells from four animals in each group). Although the possibility of bias may have been introduced in the NeuroLucida and Sholl analyses of a relatively small number of OPCs, it is evident that OPCs were shrunken following BoNT/A, with very little variation, and these measurements are corroborated by the atrophy of OPC process domains based on a much larger number of cells demonstrated in Figure 2. Together, the morphological analyses show that OPC shrinkage is a key feature following synaptic silencing with BoNT/A and is mainly due to process retraction and an evident decrease in branching.

4 | DISCUSSION

An important feature of OPCs is that they form synapses with neurones and sense neuronal synaptic activity (Bergles et al., 2000). Here, we show that BoNT/A, which silences synaptic activity in the hippocampus, results in a decrease in OPC numbers and cellular atrophy. Notably, similar changes in OPCs are associated with synaptic dysregulation in AD-like pathology in mice (Chacon-De-La-Rocha et al., 2020; Vanzulli et al., 2020). The results support a role for synaptic signaling in maintaining adult OPC numbers and integrity, which is relevant to neuropathologies in which neuronal activity is altered, such as AD, MS, and traumatic injury, as well as age-related cognitive decline.

BoNT/A is a member of the family of botulinum neurotoxins (BoNTs A–G) that inhibit neurotransmission by blocking vesicular neurotransmitter release (Caleo & Restani, 2018). BoNTs enter presynaptic terminals mainly via activity-dependent synaptic endocytosis and cleave proteins of the SNARE complex, which is necessary for synaptic vesicle fusion (Verderio et al., 2006). It has been demonstrated that infusion of BoNT/A into the mouse hippocampus cleaves SNAP-25 and prevents neuronal synaptic activity in the CA1 area (Antonucci et al., 2008). It is possible that BoNT/A cleaves SNAP-25 in OPCs, but in the hippocampus SNAP-25 is concentrated

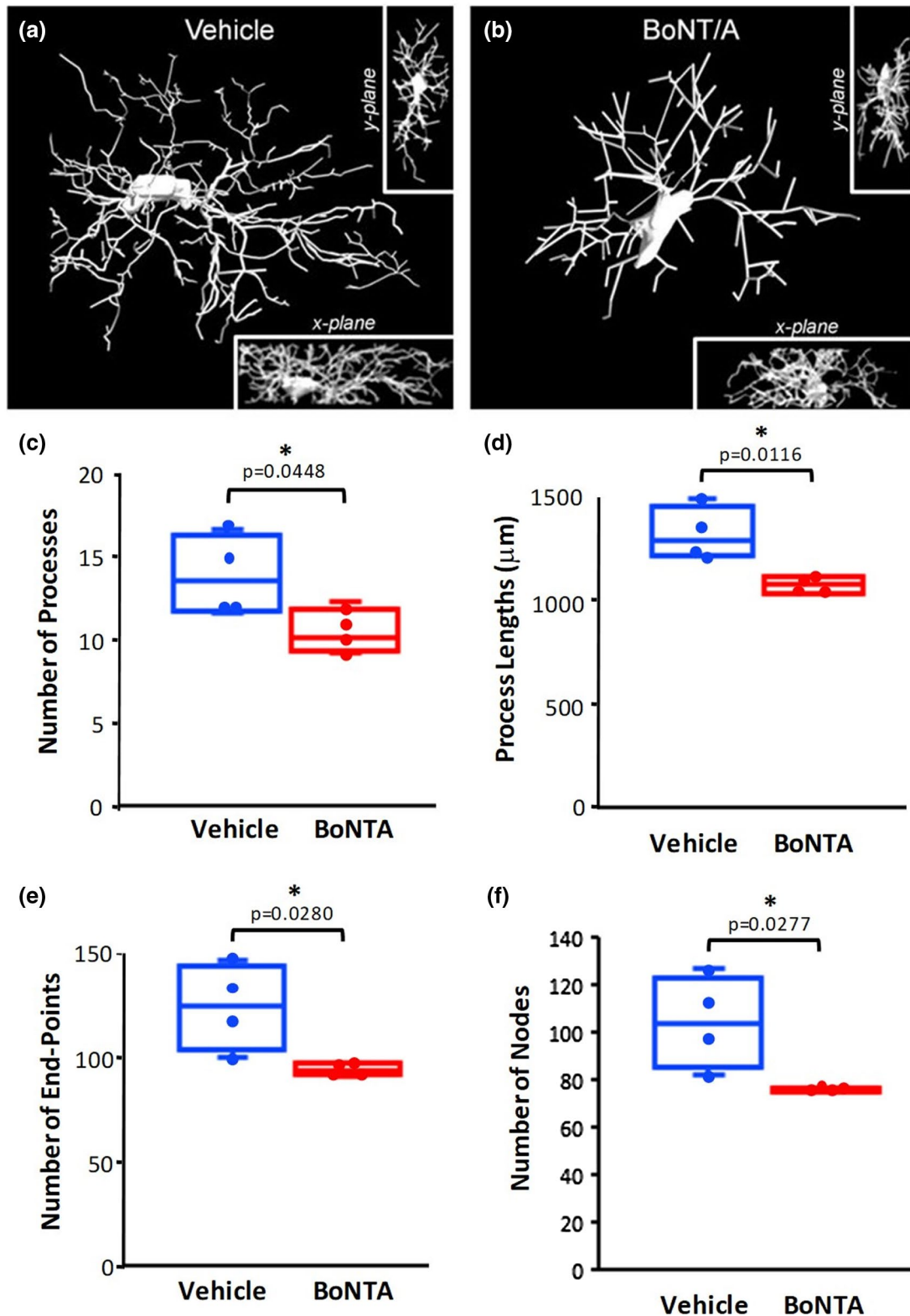


FIGURE 3 Effects of synaptic silencing with BoNT/A on OPC morphology in the adult hippocampus. Confocal images of hippocampus sections were immunolabeled for NG2 following injection with BoNT/A to silence synaptic activity, or vehicle in controls. (a, b) Confocal images were analyzed using NeuroLucida 360 (MBF Bioscience), to generate 3D images (main panels in a, b); insets illustrate the cell in the x- and y-planes. (c–f) Box-whisker plots of the number of processes per cell (c), process lengths (d), number of process terminals, or end points (e), and the number of branch points, or nodes (f). Data were from three cells drawn from the center of the CA1 field in one section per mouse, which was averaged in each mouse, to provide a mean \pm SEM from $n = 4$ animals per treatment group; p values as indicated, from unpaired t tests [Color figure can be viewed at wileyonlinelibrary.com]

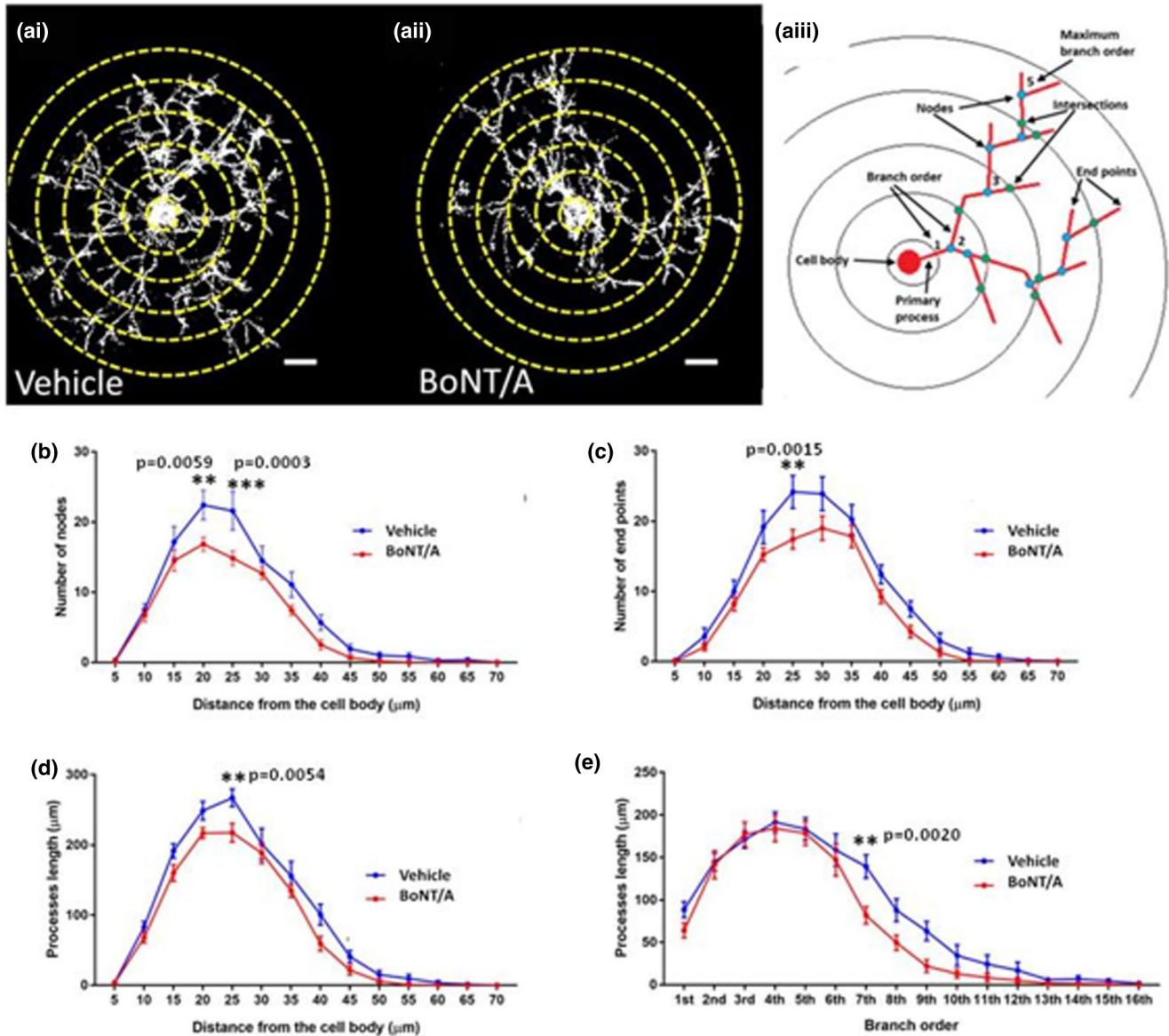


FIGURE 4 Sholl analysis of OPC process morphology in the adult hippocampus following synaptic silencing with BoNT/A. (a) Isosurface rendering to illustrate 3D morphology of OPCs (generated with Volocity software, PerkinElmer), obtained following NG2 immunolabeled cells in CA1 area of the hippocampus following injection of BoNT/A (ai) or vehicle (aii). The schematic representation in (aiii) illustrates parameters measured, where the concentric circles (termed Sholl shells) are placed at 5 µm apart, with the cell body in the middle (yellow lines in ai, aii); the points of process branching are termed nodes (blue dots), and the points where the processes intersect the Sholl shells are termed intersections (green dots) (adapted from Sholl (1953) and Rietveld et al. (2015)). (b–e) Graphs of the number of nodes or branch points (b), number of process terminals or end points (c), processes lengths (d), and length of processes of different branch orders (e). Data are mean ± SEM; n = 12 cells from four animals per group (three cells per section, taken from the center of the CA1 field); p values as indicated, from two-way ANOVA followed by Sidak’s multiple comparisons test [Color figure can be viewed at wileyonlinelibrary.com]

in neuronal terminals and is largely absent from glial processes (Schubert et al., 2011), and transcriptomic data indicate that SNAP-25 is barely detectable in OPCs and other glia, compared to neurons (Figure S1; (Zhang et al., 2014)). Glia can express SNAP-23 (Feldmann et al., 2009; Hepp et al., 1999; Schardt et al., 2009; Schubert et al., 2011), but BoNT/A acts mainly on SNAP-25 and not SNAP-23 (Sikorra et al., 2016). In addition, it has been shown that BoNT/A has little effect on astrocytes (Rojewska et al., 2018), or microglia (Caleo et al., 2012), and the primary effect of BoNT/A is on synaptic signaling, with little evidence of axonal disruption (Antonucci et al.,

2008; Caleo et al., 2012). It is not discounted that BoNT/A could act on synaptic transmission by OPCs (Hamilton et al., 2010), or have other effects on OPCs unrelated to synaptic transmission, but the results of the present study are consistent with BoNT/A acting to silence neuronal synapses and cause a decrease in OPC numbers and cell shrinkage, resulting in marked loss of overall coverage of the hippocampus by OPCs.

Our data demonstrate that BoNT/A treatment resulted in a decrease in OPC numbers, indicating that OPC self-renewal is dependent on synaptic signaling. These findings support previous

studies showing OPC proliferation is respectively increased or decreased when neuronal electrical activity is stimulated (Gibson et al., 2014) or blocked (Barres & Raff, 1993). The decrease in OPCs following BoNT/A indicates their population was not replenished by self-renewal, although further studies to measure cell proliferation are required to confirm this. A novel finding of our study is that BoNT/A caused shrinkage of adult OPC *in vivo*, with a marked retraction of distal processes and decreased branching. A similar reduction in OPC process extension and branching has been reported *in vitro* in postnatal cerebellar slices following blockade of neuronal electrical activity and glutamate receptors (Fannon et al., 2015). This is in comparison to the response of OPCs to CNS insults, which is usually marked by increased process branching to give OPCs a fibrous appearance (Butt et al., 2002; Levine et al., 2001). Time-lapse imaging demonstrates that NG2⁺ OPCs processes are highly motile and respond rapidly to changes in their environment (Hughes et al., 2013). Hence, it is possible that OPC processes are retracted from silent synapses following BoNT/A treatment, resulting in decreased coverage by OPCs, which is comparable to early atrophy of OPCs observed in mouse models of AD that are characterized by synaptic dysregulation (Chacon-De-La-Rocha et al., 2020; Vanzulli et al., 2020). The overall extent of synaptic disruption in neuropathology is unlikely to be as extensive as that of the hippocampus following BoNT/A injection, and the changes observed in the present study are more likely to reflect those that occur focally within lesions. Indeed, changes in OPC morphology are characteristic of neuropathology in human AD and MS, as well as mouse models of these diseases (Butt & Dinsdale, 2005; Dong et al., 2018; Levine & Reynolds, 1999; Li et al., 2013; Nielsen et al., 2013; Reynolds et al., 2002; Zhang et al., 2019). These data support evidence that synaptic signaling regulates adult OPC morphology and the maintenance of their numbers.

The effects of BoNT/A on hippocampal OPCs may be due mainly to blockade of glutamatergic synapses, since BoNT/A has been shown to act preferentially on excitatory synapses (Antonucci et al., 2008; Caleo et al., 2012), which are contacted by OPCs (Bergles et al., 2000). Furthermore, neurotransmitters released at synapses or along axons would also activate non-synaptic receptors on adult OPCs through what is termed volume transmission (Kula et al., 2019; Vélez-Fort et al., 2010; Hamilton et al., 2010), which would also be blocked by BoNT/A. Glutamatergic signaling has been shown to promote OPC proliferation (Chen et al., 2018; Wake et al., 2011), hence blockade of glutamate release by BoNT/A would result in the observed decline in OPC numbers. To confirm this unequivocally will require comprehensive electrophysiological, immunohistochemical, EM, cell proliferation, and fate-mapping studies. Nonetheless, we demonstrate that BoNT/A causes cleavage of SNAP-25 in our model (Figure 1), which is essential for synaptic vesicular release of glutamate (Caleo & Restani, 2018). In contrast, electrophysiological and EM studies indicate BoNT/A does not affect GABAergic synapses when used

in the hippocampal model (Antonucci et al., 2008; Caleo et al., 2012), which has been explained by the fact that SNAP-25 is expressed only at very low levels in GABAergic synapses (Verderio et al., 2004). Furthermore, although OPCs in the hippocampus receive synaptic inputs from GABAergic neurones (Bergles et al., 2000; Lin & Bergles, 2004), their blockade is reported to increase OPC numbers *in vitro* in cortical slices (Hamilton et al., 2017; Zonouzi et al., 2015), which is opposite to that observed following synaptic silencing. Also, as noted above, OPC disruption following BoNT/A *in vivo* is mirrored by blockade of glutamatergic signaling *in vitro* in cerebellar slices (Fannon et al., 2015). Thus, the balance of evidence indicates excitatory synaptic signaling plays an important role in maintaining OPC numbers and integrity in the adult hippocampus.

5 | CONCLUSIONS

This study demonstrates that the synaptic blocker BoNT/A has a major negative impact on adult OPCs, which have the fundamental function of life-long generation of oligodendrocytes. It will be of considerable interest in future studies to determine whether synaptic blockade has longer term effects on myelination that is required for the formation of new neuronal connections and learning (McKenzie et al., 2014; Xiao et al., 2016). Notably, disruption of OPCs has been shown to result in impaired myelination in aging (Neumann et al., 2019; Rivera et al., 2021), and this is a key factor in the age-related decline in cognitive function (Bartzokis, 2004), as well as the failure of remyelination in chronic MS (Sanai et al., 2016), and the accelerated loss of myelin observed in AD (Nasrabad et al., 2018; Vanzulli et al., 2020). In conclusion, disruption of OPCs following synaptic blockade in the hippocampus is relevant to cognitive function and neuropathologies where there is dysregulation of neuronal synaptic activity.

DECLARATION OF TRANSPARENCY

The authors, reviewers and editors affirm that in accordance to the policies set by the *Journal of Neuroscience Research*, this manuscript presents an accurate and transparent account of the study being reported and that all critical details describing the methods and results are present.

ACKNOWLEDGMENTS

We thank Dr Olivier Raineteau for assistance and use of NeuroLucida in the INSERM Stem Cell and Brain Research Institute, Univ Lyon, France. The research presented in this paper was supported by grants from the BBSRC (AB, Grant Number BB/M029379/1), MRC (AB, Grant Number MR/P025811/1), Alzheimer's Research UK (DG-N, AB, Grant Number PG2014B-2), University of Portsmouth PhD Programme (AB, ICR), and CNR - Joint Laboratories (MC, LR).

- dynamics in the healthy adult CNS: Evidence for myelin remodeling. *Neuron*, 77(5), 873–885. <https://doi.org/10.1016/j.neuron.2013.01.006>
- Zawadzka, M., Rivers, L. E., Fancy, S. P. J., Zhao, C., Tripathi, R., Jamen, F., Young, K., Goncharevich, A., Pohl, H., Rizzi, M., Rowitch, D. H., Kessler, N., Suter, U., Richardson, W. D., & Franklin, R. J. M. (2010). CNS-resident glial progenitor/stem cells produce Schwann cells as well as oligodendrocytes during repair of CNS demyelination. *Cell Stem Cell*, 6(6), 578–590. <https://doi.org/10.1016/j.stem.2010.04.002>
- Zhang, P., Kishimoto, Y., Grammatikakis, I., Gottimukkala, K., Cutler, R. G., Zhang, S., Abdelmohsen, K., Bohr, V. A., Misra Sen, J., Gorospe, M., & Mattson, M. P. (2019). Senolytic therapy alleviates A β -associated oligodendrocyte progenitor cell senescence and cognitive deficits in an Alzheimer's disease model. *Nature Neuroscience*, 22(5), 719–728. <https://doi.org/10.1038/s41593-019-0372-9>
- Zhang, Y., Chen, K., Sloan, S. A., Bennett, M. L., Scholze, A. R., O'Keefe, S., Phatnani, H. P., Guarnieri, P., Caneda, C., Ruderisch, N., Deng, S., Liddelow, S. A., Zhang, C., Daneman, R., Maniatis, T., Barres, B. A., & Wu, J. Q. (2014). An RNA-sequencing transcriptome and splicing database of glia, neurons, and vascular cells of the cerebral cortex. *The Journal of Neuroscience*, 34(36), 11929–11947. <https://doi.org/10.1523/JNEUROSCI.1860-14.2014>
- Ziskin, J. L., Nishiyama, A., Rubio, M., Fukaya, M., & Bergles, D. E. (2007). Vesicular release of glutamate from unmyelinated axons in white matter. *Nature Neuroscience*, 10(3), 321–330. <https://doi.org/10.1038/nn1854>
- Zonouzi, M., Scafidi, J., Li, P., McEllin, B., Edwards, J., Dupree, J. L., Harvey, L., Sun, D., Hübner, C. A., Cull-Candy, S. G., Farrant, M., & Gallo, V. (2015). GABAergic regulation of cerebellar NG2 cell development is altered in perinatal white matter injury. *Nature Neuroscience*, 18(5), 674–682. <https://doi.org/10.1038/nn.3990>

SUPPORTING INFORMATION

Additional Supporting Information may be found online in the Supporting Information section.

FIGURE S1 Visualization of SNAP-25 mRNA expression in OPCs compared to neurons and other glia, from Transcriptomic data sets generated by Zhang et al., 2014. Adapted from www.brainrnaseq.org Transparent Peer Review Report

Transparent Science Questionnaire for Authors

How to cite this article: Chacon-De-La-Rocha I, Fryatt GL, Rivera AD, et al. The synaptic blocker botulinum toxin A decreases the density and complexity of oligodendrocyte precursor cells in the adult mouse hippocampus. *J Neurosci Res*. 2021;99:2216–2227. <https://doi.org/10.1002/jnr.24856>